Pergamon

Bioorganic & Medicinal Chemistry 6 (1998) 2245–2260

BIOORGANIC & MEDICINAL CHEMISTRY

Ligand Binding to I_2 Imidazoline Receptor: The Role of Lipophilicity in Quantitative Structure–Activity Relationship Models

M. Pigini,[a] P. Bousquet,[b] L. Brasili,[c] A. Carrieri,[d] R. Cavagna,[b] M. Dontenwill,[b] F. Gentili,[a] M. Giannella,[a] F. Leonetti,[d] A. Piergentili,[a] W. Quaglia[a] and A. Carotti[d,*]

[a]*Dipartimento di Scienze Chimiche, Università di Camerino, Via S. Agostino 1, 62032 Camerino (MC), Italy*
[b]*Laboratoire de Pharmacologie Cardiovasculaire et Rénale, Université Louis Pasteur, CNRS URA 589, Faculté de Médicene, 11 rue Humann, 67000 Strasbourg, France*
[c]*Dipartimento di Scienze Farmaceutiche, Università di Modena, via Campi 183, 41100 Modena, Italy*
[d]*Dipartimento Farmaco-Chimico, Università degli Studi, via E. Orabona 4, 70125 Bari, Italy*

Received 8 April 1998; accepted 25 May 1998

Abstract—A series of 2-*trans*-styryl-imidazoline (*tracizoline*) congeners were designed and tested to develop 2-D and 3-D QSAR models for their binding to imidazoline (I_2) receptor. The important role of lipophilicity was assessed by classical 2-D QSAR study (Hansch approach) and by comparative molecular field analysis (CoMFA) with the inclusion of the molecular lipophilicity potential (MLP), as an additional descriptor, besides standard steric and electrostatic fields. Results from these studies were compared to those obtained in a previous modeling study of I_2 receptor ligands and integrated into a new, comprehensive model, based on about sixty I_2 receptor ligands. This model revealed, at the three-dimensional level, the most significant steric, electrostatic, and lipophilic interactions accounting for high I_2 receptor affinity.

Introduction

Imidazoline binding sites (IBS) or imidazoline/guanidinium receptive sites (IGRS), different from those of classical α-adrenoceptors, recognize bioactive endogenous ligands and a variety of exogenous compounds containing imidazoline or guanidinium moieties.[1–3] Since the various IBS differ in their ligand properties, tissue distribution, subcellular localization, and structural features, they constitute a heterogeneous family of proteins. Based on the rank order of affinity for different ligands, IBS have been classified in two major classes, I_1 and I_2 receptors, which traditionally have been labeled with [^{3}H]-Clonidine and [^{3}H]-Idazoxan, respectively.[4] Further evidences from ligand binding studies has led to the division of I_2 receptor into two subtypes, I_{2A} and I_{2B}, according to their high or low affinity for amiloride, respectively.[5]

IBS ligands may elicit several important functional effects such as decrease of blood[6] and intraocular pressure,[7] increase of protein synthesis in astrocytes,[8] increase of insulin[9] and gastric acid secretion,[10] inhibition of sodium reabsorption in renal tubules,[11] inhibition of neurotransmitter release,[12] inhibition of ion flux in 5-HT_3 receptor,[13] and finally modulation of food intake.[14]

However, despite the recent advances in the search of the physiological[15] and therapeutical effects of IBS ligands,[16] a conclusive receptor (sub)classification and a definition of the putative physiopathological role of IBS have yet to be assessed, mainly, because the ligands used for their characterization often suffered from lack of selectivity with respect to α-adrenoceptors.

Key words: Imidazoline receptor; Pharmacophore model; Quantitative structure–activity relationships; Comparative molecular field analysis.
*Corresponding author: Fax: ++3980.5442724; E-mail: carotti@farmchim.uniba.it

0968-0896/98/$ - see front matter
PII: S0968-0896(98)00182-5

In this context, a few years ago we began a systematic study aimed at the discovery of new imidazoline receptor ligands endowed with high affinity and selectivity toward I_2 receptor subtype. Two ligands, namely *benazoline* **1** and *tracizoline* **2** (Chart 1), with outstanding affinity and unprecedented selectivity for I_2 receptor, have been discovered.[17,18] A subsequent modeling study led us to propose informative bi- and three-dimensional models able to interpret both the binding affinity and the I_2/α_2 selectivity of the examined ligands.[19]

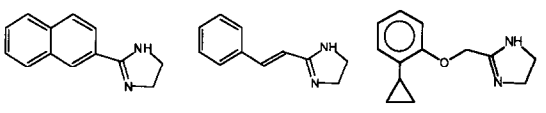

Chart 1.

The congruent 2-D and 3-D-QSAR results from such a study allowed us to find out, within the topological and physicochemical space analyzed, the key structural features governing the ligand binding. However, several regions, especially the ones around the aromatic moieties linked to the imidazoline ring through an aliphatic bridge, have not been properly explored yet due to some intrinsic limitations of available data sets. In particular, the determinant *ortho* region has been explored mainly in steric terms on a series of *ortho*-substituted phenoxy congeners, structurally related to *cirazoline* **3**, and no systematic study of the *para* region has been carried out. Moreover, the nature of analyzed data set did not allow us to ascertain, with a sufficient degree of confidence, the influence of the lipophilicity on the ligand binding. Therefore, we decided to design and test a new series of imidazoline derivatives aiming at assessing the role of lipophilicity in the ligand binding to I_2 receptor and at completing, improving and refining our former 3-D models.

Tracizoline **2** was selected as the lead compound and both traditional Hansch[20] analysis and Comparative Molecular Field Analysis (CoMFA)[21] were used for quantitative data examination.

The combined Hansch (2-D QSAR) and CoMFA (3-D QSAR) methods have been successfully applied by us[22–24] and others[25,26] to the study of several important physicochemical and biological processes. Very often, findings from 2-D QSAR have given information complementary to that obtained by 3-D QSAR methods leading to an improved physicochemical interpretation of the structure–activity relationship models.

Chemistry

Compounds **4–24** were synthesized according to standard methods by condensation of suitable methyl cinnamates with ethylenediamine in the presence of $Al(CH_3)_3$ or by condensation of the appropriate aromatic aldehydes with 2-methyl-2-imidazoline (Scheme 1). Only the *trans* isomers were isolated from the reaction mixtures. Amino derivatives **9** and **17** were prepared by catalytic hydrogenation over Nickel-Raney of the corresponding nitro compounds **7** and **18**, respectively.

Compounds **40** and **41** (Chart 2), carrying an aliphatic substituent in place of an aromatic ring, were synthesized by similar procedures from the corresponding methyl acrylates. The *ortho*-methyl phenethyl congener **42** (Chart 2) was similarly synthesized from the suitable methyl propionate.

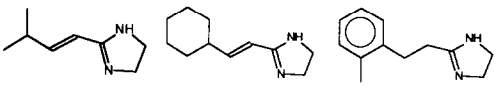

40
pKi: $I_2 = 6.57 \pm 0.07$;
pKi: $\alpha_2 = 5.21 \pm 0.07$

41
pKi: $I_2 = 7.26 \pm 0.25$;
pKi: $\alpha_2 = 5.43 \pm 0.1$

42
pKi: $I_2 = 8.37 \pm 0.04$;
pKi: $\alpha_2 = 5.21 \pm 0.02$

Chart 2.

Results and Discussion

Structure–activity relationships (SAR)

Most of the newly synthesized compounds displayed a high affinity for I_2 receptor and a much lower affinity for α_2 adrenoceptor. As a consequence, analogously to the reference compound **2**, high I_2/α_2 selectivity ratios were in general observed (Table 1).

All the *para* substituted congeners showed an affinity lower than parent compound **2**. Conversely, a higher affinity was observed for some *ortho*-substituted derivatives, namely **5** and **10**. The former displayed the highest I_2 affinity, with a pK_i value better than the prototype **2** (9.43 versus 8.74), and a high selectivity ratio ($I_2/\alpha_2 = 2.455$).

Interestingly, the only *meta* derivative **11** synthesized so far showed a high I_2 affinity ($pK_i = 9.05$). Substitution of the phenyl ring of **2** with nitrogen heterocycles (**19, 20**) or with alkyl groups (**40, 41**), diminished the I_2 affinity, whereas, ligands with oxa (**21**) and sulfur (**22**) heterocycles retained a high affinity. The isomeric naphthyl derivatives **23** and **24**, displayed quite diverse I_2 affinities as observed in the past with similar I_2 ligands bearing planar, polycyclic aromatic moieties.[18]

As far as the α_2 adrenoceptor activity is concerned, all the ligands had very low affinity and no particular structure–activity relationships emerged. However, it is worth noting that, with the exception of the amino congener **9**, *ortho*-substituted derivatives showed an α_2 adrenoceptor activity greater than the corresponding *para* congeners.

Quantitative structure–activity relationships (QSAR)

Firstly, the congeneric tracizolines (**2, 4–18**) were subjected to classical QSAR analysis using a cross-validated multilinear regression technique according to the Hansch approach.[20] To gain more valuable physicochemical insight at the topological level, the *ortho* and *para* substituted congeners were analyzed separately. Classical steric (molar refractivity, MR; Charton, ν), electronic (Hammett, σ; Field, F and Resonance, R) and lipophilic (Hansch, π) substituent constants were taken from standard compilations[28] and used as physicochemical descriptors (independent variables). The best one-variable equations for the *ortho* and *para* subsets were, respectively:

$$\begin{gathered} pK_i = 0.60\ (\pm 0.20)\pi + 8.59\ (\pm 0.12) \\ n = 8,\ r^2 = 0.596,\ s = 0.353 \end{gathered} \quad (1)$$

$$\begin{gathered} pK_i = -1.15\ (\pm 0.44)F + 5.51\ (\pm 0.15) \\ n = 8,\ r^2 = 0.530,\ s = 0.269 \end{gathered} \quad (2)$$

where K_i is the inhibition constant, n is the number of data points, r is the correlation coefficient, and s is the standard deviation from regression. Standard errors are reported in parentheses.

Equation (1) and eq (2) are not so good in statistical terms but can be considered as indicative of different physicochemical interactions in the *ortho* and *para* regions. In the former, a lipophilic interaction seems to take place, whereas, an electronic interaction, most likely governed by a localized field effect, seems to be involved in the *para* region. For the *para* substituents much improved statistics were obtained by eliminating one strong outlier, namely the hydroxy congener **16** ($r^2 = 0.771, s = 0.129$); no correlation was found neither with the electronic constants R and σ nor with the lipophilic constant π.

This last observation suggests that a specific lipophilic interaction should take place only in the *ortho* region and that ligand binding is not influenced by the overall molecular lipophilicity. To further prove this hypothesis the QSAR analysis was performed also on the heterocyclic derivatives **19–22** (with the inclusion of **2**) which should place their heteroatoms into the *ortho* region. The following correlation equation was formulated:

$$\begin{gathered} pK_i = 0.74\ (\pm 0.56)\pi' + 7.35\ (\pm 0.74) \\ n = 5,\ r^2 = 0.857,\ s = 0.256 \end{gathered} \quad (3)$$

In eq (3), π′ values were estimated by C-log P[27] and refer to the whole heterocyclic substituent (see Table 1). Even though eq (3) cannot be directly compared with eq (1) (the lipophilicity is expressed with different π values) it clearly confirms the relevant, positive contribution of the lipophilicity to the receptor binding in the *ortho* region. By expressing the lipophilicity of the *ortho*-substituted and heterocyclic tracizoline congeners in a homogeneous way, that is considering the π values of the R-C_6H_4 and heterocyclic moieties, eqs (2) and (3) can be merged into the single eq (4):

$$\begin{gathered} pK_i = 0.61\ (\pm 0.12)\pi' + 7.43\ (\pm 0.48) \\ n = 12,\ r^2 = 0.713,\ s = 0.316,\ q^2 = 0.505 \end{gathered} \quad (4)$$

where q is the cross-validated correlation coefficient. Equation (4) presents satisfactory statistical parameters both as fitting (r^2 and s) and predictive power (q^2).

The QSAR analysis of the strictly congeneric series of tracizolines (cps **2, 4–22**) unrevealed the key role of the lipophilic interactions in the *ortho* region, whereas a different and less important binding, mainly of electronic nature, was detected in the *para* region.

Our past modeling study,[19] performed by the same methodological approach on a different set of I_2 receptor ligands, was not able to find out the lipophilic nature of the interaction in the *ortho* region. In particular, for the series of cirazoline congeners reported in Table 2 (compds **3, 25–35**), that should place their substituents in the same *ortho* space of tracizolines, the following equation has been proposed:

$$\begin{gathered} pK_i = -1.07\ (\pm 0.45)MR + 9.60\ (\pm 0.78) \\ n = 12,\ r^2 = 0.738,\ s = 0.530 \end{gathered} \quad (5)$$

where MR is the substituent molar refractivity. An equation with similar statistics ($r^2 = 0.732, s = 0.536$) could be obtained by substituting MR with the van der Waals volume. These findings suggested a limited receptor accessibility in the *ortho* space, the most active compounds being those bearing small-sized substituents.

The contrasting indications about the nature of the ligand binding in the *ortho* space coming from the QSAR analysis of tracizolines (eqs (3) and (4)) and cirazolines (eq (5)) could be ascribed to the particular nature and composition of the cirazoline data set (compds **3, 25–35** in Table 2) which had been designed to study the ligand binding mostly in steric terms. In the light of the present results, the QSAR of cirazolines were reexamined and, in order to have a straightforward comparison with eq (4) from tracizolines, the π′ values referred to the R-C_6H_4 moieties were taken into account.

Table 1. I_2 and α_2 receptors affinity data[a] and physicochemical descriptors[b] of Tracizoline analogues

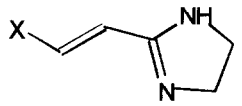

X =) (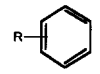 ; Het) (Ar

Compd	R	pK_i I_2	pK_i α_2	π	π′	F	Ref
2	H (*Tracizoline*)	8.74 ± 0.08	4.85 ± 0.09	0.00	1.95	—	
4	2-Cl	8.54 ± 0.15	5.66 ± 0.09	0.71	2.66	—	
5	2-CH_3	9.43 ± 0.21	6.04 ± 0.11	0.56	2.51	—	
6	2-CH_3O	8.24 ± 0.13	6.40 ± 0.12	−0.02	1.93	—	
7	2-NO_2	8.69 ± 0.18	5.49 ± 0.08	−0.28	1.67	—	
8	2-OH	7.97 ± 0.12	5.64 ± 0.04	−0.67	1.98	—	45
9	2-NH_2	7.90 ± 0.08	4.60 ± 0.09	−1.23	0.72	—	
10	2-N_3	8.96 ± 0.07	5.57 ± 0.10	0.46	2.41	—	
11	3-CH_3	9.05 ± 0.11	6.96 ± 0.12				
			4.96 ± 0.07	—	—	—	
12	4-Cl	8.22 ± 0.09	5.10 ± 0.07	—	2.66	0.42	
13	4-I	8.17 ± 0.15	5.00 ± 0.06	—	3.07	0.42	
14	4-CH_3	8.54 ± 0.14	5.17 ± 0.06	—	2.51	0.01	
15	4-CH_3O	8.00 ± 0.12	5.08 ± 0.08	—	1.93	0.65	
16	4-OH	7.61 ± 0.16	5.28 ± 0.07	—	1.98	0.33	45
17	4-NH_2	8.37 ± 0.19	5.01 ± 0.11	—	0.72	0.08	
18	4-NO_2	7.89 ± 0.09	4.30 ± 0.02	—	1.67	0.65	46
Compd	**Het**	**pK_i I_2**	**pK_i α_2**	**π**	**π′**	**F**	
19	2-Pyridyl	8.03 ± 0.12	4.46 ± 0.11	—	0.60	—	
20	2-Pyrrolyl	7.27 ± 0.09	5.33 ± 0.10	—	0.24	—	
21	2-Furyl	8.52 ± 0.06	5.29 ± 0.08	—	1.27	—	47
22	2-Thienyl	8.50 ± 0.08	5.73 ± 0.07	—	1.74	—	48
Compd	**Ar**	**pK_i I_2**	**pK_i α_2**	**π**	**π′**	**F**	
23	1-Naphthyl	8.21 ± 0.09	6.29 ± 0.09	—	—	—	
24	2-Naphthyl	7.69 ± 0.13	6.70 ± 0.13	—	—	—	
			4.86 ± 0.08				

[a]Expressed as $pK_i \pm SD$.
[b]Only data used for the derivation of regression eqs (1)–(4) and eqs (8)–(10) are listed.

The following equation was derived:

$$pK_i = -1.09\ (\pm 0.33)\pi' + 11.48\ (\pm 1.11)$$
$$n = 12, r^2 = 0.516, s = 0.721 \qquad (6)$$

The unsatisfactory statistics of eq (6), which had led us to prefer eq (5) with MR, was significantly improved by eliminating a strong outlier, that is the isopropoxy congener **35**, from the regression:

$$pK_i = -1.29\ (\pm 0.27)\pi' + 12.26\ (\pm 0.89)$$
$$n = 11, r^2 = 0.723, s = 0.553 \qquad (7)$$

Incidentally, the isopropoxy was the only alkoxy substituent present in the cirazoline data set. Taken together, eqs (4) and (7), contribute to a better understanding of the interaction in the *ortho* region, being based on substituents which spanned a quite large and diverse physicochemical space. In fact, only apparently the different sign with π′ in the two equations is contradictory, since they describe two different sides of the same interaction: the favorable lipophilic interaction of the tracizoline *ortho* substituents and the unfavorable (lipophilic–steric) interaction of the relatively larger *ortho* substituents of cirazolines. In other words, a classical parabolic (or bilinear) model with π′ would result from the merging of cirazolines and tracizolines into a single data set (cps **2–10, 19–22**, and **25–35**). Indeed, the development of eq (8) confirmed such a hypothesis:

Table 2. I_2 and α_2 receptors affinity data[a] and physicochemical descriptors[b] of Cirazoline analogues

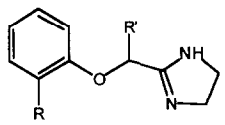

Compd	R	R'	pK_i I_2	pK_i α_2	π'^c	MR	vdW'[c]
3	cC_3H_5	H	8.41	7.77	3.09	1.35	111.3
25	H	H	9.04	7.28	1.95	0.10	71.7
26	CH_3	H	9.05	5.39	2.51	0.56	88.2
27	CH_2CH_3	H	8.57		2.97	1.03	104.4
28	$CH(CH_3)_2$	H	8.66	6.59	3.48	1.50	120.4
29	$C(CH_3)_3$	H	6.70		3.93	1.96	136.8
30	$CH_2CH_2CH_3$	H	8.21		3.50	1.50	120.3
31	CH_2-$CH=CH_2$	H	8.85		3.05	1.45	113.6
32	CH_2-C_6H_5	H	6.70	6.52	3.96	3.00	152.6
33	$CH(CH_3)CH_2CH_3$	H	7.30		3.91	1.96	136.3
34	C_6H_5	H	6.52	7.10	3.91	2.54	136.8
35	$OCH(CH_3)_2$	H	7.07		2.71	1.71	127.5
36	H	CH_3	5.57	7.01	—	0.10	—
37	CH_3	CH_3	6.70		—	0.56	—
38	$CH(CH_3)_2$	CH_3	5.29		—	1.50	—
39	$OCH(CH_3)_2$	CH_3	5.62		—	1.71	—

[a]See Table 1.
[b]Only data used for the derivation of regression eqs (5) (10) are listed.
[c]Referred to the C_6H_4-R group.

$$pK_i = 2.07\ (\pm 0.86)\pi' - 0.50\ (\pm 0.18)\pi'^2 + 6.67\ (\pm 0.91)$$
$$n = 24,\ r^2 = 0.634,\ s = 0.521 \qquad (8)$$

Again, the isopropoxy congener **35** was a strong outlier; its elimination led to eq (9) which presents markedly better statistics:

$$pK_i = 2.30\ (\pm 0.67)\pi' - 0.55\ (\pm 0.14)\pi'^2 + 6.51\ (\pm 0.70)$$
$$n = 23,\ r^2 = 0.778,\ s = 0.399,\ q^2 = 0.705,\ \pi'_o = 2.10 \qquad (9)$$

In eq (9), π'_o indicates the value of the lipophilic substituent constant to which it should correspond the highest affinity. This value is quite near to the observed experimental values. A bilinear model, described by the following equation, was also obtained:

$$pK_i = 0.69\ (\pm 0.21)\pi' - 7.87\ (\pm 1.50)\log(\beta\pi' + 1) + 7.39\ (\pm 0.41)$$
$$n = 23,\ r^2 = 0.873,\ s = 0.309,\ q^2 = 0.832,$$
$$\pi'_o = 2.70,\ \mathrm{Log}\beta = -3.72 \qquad (10)$$

Eq (10) shows significantly improved statistics over eq (9) but the coefficients of linear and bilinear terms are markedly dissimilar and moreover the optimum of lipophilicity ($\pi'_o = 2.70$) is higher than experimental data. For these reasons the parabolic eq (9) should be considered a more appropriate model for the description of the SAR of *ortho*- substituted ligands. Both eqs (9) and (10), point out the key role of lipophilic interaction in the *ortho*- region and clearly suggest that an increasing lipophilicity up to a π' value near 2.10 favors the ligand binding. Substituents with higher lipophilicity (or larger size) do not fit the lipophilic *ortho* region of the receptor and as a consequence the affinity decreases as the lipophilicity (or size) of the substituent increases. Similar results have been often found in several studies of enzyme-ligand interactions.[29,30]

3-D QSAR study: comparative molecular field analysis

The valuable indications coming from the preceding QSAR analyses were critically examined in comparison to the 3-D models derived earlier by means of Comparative Molecular Field Analysis (CoMFA).[19] CoMFA[21] is a widely used tool for studying quantitative structure–activity (property) relationships (QSAR, QSPR)[31] at the three-dimensional level. Unlike the traditional Hansch analysis, which makes use of substituent parameters, CoMFA relates the biological activity (target property) of a series of molecules with their steric and electrostatic fields sampled at grid points defining a large 3-D box around the molecule. CoMFA columns (descriptors) are commonly constituted by the steric (Lennard–Jones) and electrostatic (Coulomb)

potentials computed for each molecule, at each grid point, by means of a suitable probe, usually, an sp^3 carbon atom with a charge of +1. Partial Least Squares (PLS)[32] is used as the regression method to develop the relationship between independent variables (steric and electrostatic potentials) and biological activity (dependent variable). PLS analysis produces model equations which explain the variance in the target property in terms of the independent variables.[33] The optimum number of components (latent variables) is determined by cross-validation and the model predictive ability is assessed by cross-validated r^2 (r^2_{cv}, q^2).[34] The graphical representation of CoMFA results (isocontour maps) indicated the regions where the variation in steric and electrostatic properties of different molecules in a data set is correlated with the variation of biological activity. Even though much care has to be used to avoid an over interpretation of the isocontour maps in the definition of the binding site topology, no doubt the CoMFA graphs may be taken as a useful indication to guide future synthesis and to develop sound hypotheses on the nature of putative ligand–receptor interactions.

As just discussed, classical 3-D QSAR studies based on CoMFA rely on standard steric and electrostatic molecular fields to model receptor–ligand interactions. Unfortunately, as demonstrated in several QSAR investigations,[35] these two fields are not able to appropriately describe all binding forces. Furthermore, CoMFA describes only the enthalpic component of the ligand–receptor interactions. Introducing the molecular lipophilicity potential (MLP)[36] as an additional field has been shown to significantly improve the descriptive, predictive and interpretative power of CoMFA in many cases.[37] The MLP encodes indeed hydrogen bonds and hydrophobic interactions not sufficiently described by the steric and electrostatic fields and includes also an entropy component.[38] For these reasons, the CoMFA methodology, with the inclusion of the MLP, was selected as an appropriate tool to study the SAR of imidazoline receptor ligands.

Molecular models were constructed from the fragment library of SYBYL 6.3 and optimized by the AM1 Hamiltonian within the suite of program MOPAC.[39]

Table 3. Statistical results of CoMFA for Tracizoline derivatives **2, 4–9, 19–22** (11 ligands)

Model	Field(s)	q^{2a}	ONC[b]	r^{2c}	s^d	F[e]	Ste[f]	Ele[f]	Lipo[f]
T1	ste	−0.471	1	—	—	—	100		
T2	ele	−0.495	1	—	—	—		100	
T3	lipo	0.636	2	0.858	0.237	24.10			100
T4	ste + lipo	−0.660	1						
T5	ste + lipo	0.449	3	—	—	—			
T6	ele + lipo	0.408	2	—	—	—			

[a]Cross-validated correlation coefficient.
[b]Number of components used in the final PLS analyses corresponding to the first maximum of the function $q^2 = f(N)$ in cross-validated analysis.
[c]Correlation coefficient of the final PLS analyses.
[d]Standard error of estimate; measure of the unexplained uncertainty.
[e]F ratio; the higher the F ratio, the better the PLS analysis.
[f]Relative contribution of the steric (ste), electrostatic (ele) and lipophlic (lipo) fields in the PLS analyses.

Table 4. Statistical results of CoMFA for Cirazoline derivatives **3, 25–35** (12 ligands)

Model	Field(s)	q^{2a}	ONC[b]	r^{2c}	s^d	F[e]	Ste[f]	Ele[f]	Lipo[f]
C1	ste	0.685	2	0.949	0.246	84.02	100		
C2	ele	0.183	2	—	—	—		100	
C3	lipo	0.326	2	—	—	—			100
C4[(*)]	lipo	0.534	2	0.946	0.260	69.65			100
C5	ste + ele	0.468	2	—	—	—			
C6	ste + lipo	0.644	2	0.944	0.258	76.42	58		42
C7	ele + lipo	0.341	2	—	—	—			

*Excluding cp. **35**.
[a–f]See legend of Table 3.

According to our previous results,[19] only charged molecules were taken into account and used in the development of the present CoMFA models. For the derivation of PLS models of tracizolines (Table 3) and cirazolines (Table 4) the molecular superimpositions were made onto the *tracizoline* **2** and *cirazoline* **3**, respectively, that were chosen as the templates in their minimum energy conformation. Each ligand molecule was subjected to a conformational analysis through a systematic search and the conformers giving the best fit with the template were selected allowing an energy penalty up to 2 Kcal/mol for tracizolines and 6 Kcal/mol for cirazolines (see ref[19] for a detailed discussion on this apparently wide energy window) over the absolute minimum energy conformer. The following elements were used for the rigid fit on the corresponding atoms of the templates: all the heavy atoms of the imidazoline ring, the two heavy atoms in the bridge and all the aromatic carbons. For the overlay of mixed sets leading to models CT (cirazolines + tracizolines, Table 5) and model W (Table 6, general models including all the imidazoline ligands, not shown in Tables 1 and 2, but considered in our previous modeling study)[19] *tracizoline* **2** and *benazoline* **1**, respectively, were used as the templates, following the above alignment criteria for CT and the one reported in our previous paper (alignment a)[19] for the inclusive models W.

All the selected ligand conformations were superimposed by the RIGIDFIT option of SYBYL (poorer results always came from the FIELDFIT option) and subjected to PLS analysis in conjunction with cross-validation (CV; leave-one-out method)[40] to obtain the optimal number of components (ONC) to be used in the subsequent analyses. The PLS run was repeated with the ONC (see below) and a number of CV groups set to zero.

However, in following strictly this procedure there was a risk of obtaining overfitted models due to a relatively high value of components used.[41] We therefore chose, from a plot of the cross-validated r^2_{cv} (q^2) versus ONC, the first maximum in the curve which generally tended to reach a plateau.

This selection of a lower number of components than the ONC given by default in SYBYL generally yields poorer statistics in terms of r^2 and standard deviations (worse fitting), but more realistic and trustworthy models.[42]

PLS and CV permit to establish the optimal dimensionality of each model and thereby to derive the calibration equation with latent variables which can be converted to the original parametric space represented by probe-ligand interaction energies.

Table 5. Statistical results of CoMFA for Cirazoline + Tracizoline derivatives **2–9, 19–22, 25–35** (23 ligands)

Model	Field(s)	q^{2a}	ONC[b]	r^{2c}	s^d	F[e]	Ste[f]	Ele[f]	Lipo[f]
CT1	ste	0.369	3	—	—	—	100		
CT2	ele	−1.004	1	—	—	—		100	
CT3	lipo	0.636	3	0.895	0.288	53.77			100
CT4(*)	lipo	0.625	3	0.900	0.276	54.27			100
CT5	ste + ele	−0.055	1	—	—	—			
CT6	ste + lipo	0.559	3	0.910	0.266	63.84	54		46
CT7	ele + lipo	−0.186	3	—	—	—			
CT8	ste + ele + lipo	0.201	3	—	—	—			

*Excluding cp. **35**.
[a–f]See legend of Table 3.

Table 6. Statistical results of CoMFA for Cirazoline + Tracizoline (compds **1–39**) and other reported imidazoline derivatives[18,19] (59 ligands)

Model	Field(s)	q^{2a}	ONC[b]	r^{2c}	s^d	F[e]	Ste[f]	Ele[f]	Lipo[f]
W1	ste	0.536	5	0.826	0.456	50.33	100		
W2	ele	0.558	5	0.821	0.462	48.63		100	
W3	lipo	0.542	5	0.838	0.440	54.77			100
W4	ste + ele	0.622	4	0.836	0.438	68.93	58	42	
W5	ste + lipo	0.586	4	0.857	0.410	80.72	48		52
W6	ele + lipo	0.575	4	0.845	0.426	73.82		40	60
W7	ste + ele + lipo	0.635	5	0.886	0.369	82.27	35	26	39

[a–f]See legend of Table 3.

A 3-D QSAR equation is then produced and its coefficients multiplied by the standard deviations associated to the energy variables, can be used to draw the coefficient isocontour maps which yields a meaningful pictorial representation of CoMFA results.

For the present work a stepwise approach was devised to carry out the CoMFA studies. First the congeneric series were analyzed separately, then pooled together and finally merged with all the imidazoline ligands examined in the past studies[18,19] to develop a coherent, inclusive model. This approach has permitted a straightforward comparison with the QSAR equations (also based on congeneric compounds) and a better evaluation of the diverse contributions of the different models to the final comprehensive model.

The statistical results obtained for the different PLS models are shown in Tables 3–6 and refer to tracizolines (Models T), cirazolines (Models C), cirazolines + tracizolines (Models CT) and the whole data set (Models W), respectively. Only models W include the isomeric naphthyl congeners **23** and **24** that were designed as molecular yardsticks to map the receptor with planar ligands. CoMFA results are listed from separated and combined steric, electrostatic, and lipophilic fields.

Tables 3–6 show many statistically significant models in terms of predictive (q^2) and fitting (r^2, s) power. In this regard, it can be observed that all the retained final CoMFA models had a q^2 value well above 0.3 which corresponds to a low probability of chance correlation ($p < 0.05$, that is $< 5\%$).[31]

However, to be even safer on the potential risk of chance correlations, the biological data were reassigned randomly to the compounds and the PLS analyses were repeated.

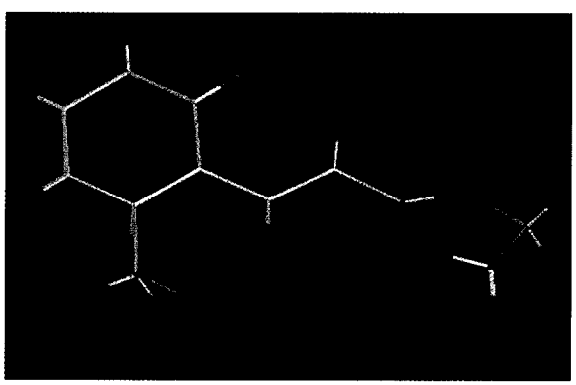

Figure 1. Lipophilic contour plot for model T3 expressed as STDEV×COEFF (contour level: −0.015 cyan; 0.038 yellow. Color code: see Table 7). Ligands **5** and **8** are displayed to help interpretation.

In no case were good predictive models obtained (q^2 always < 0.2). The results from the CoMFA study on separated and combined classes of ligands are discussed below and shown graphically in Figures 1–4 .

The isocontour maps in Figures 1–4 represent regions of space around the ligands where the variations (STDEVxCOEFF) of the considered field are the largest. The color code to characterize favorable and unfavorable zones of each field is the same used by us[22] and others[37] and it is described in Table 7. The dual interpretability of both electrostatic (variation of a positive or a negative charge) and lipophilic

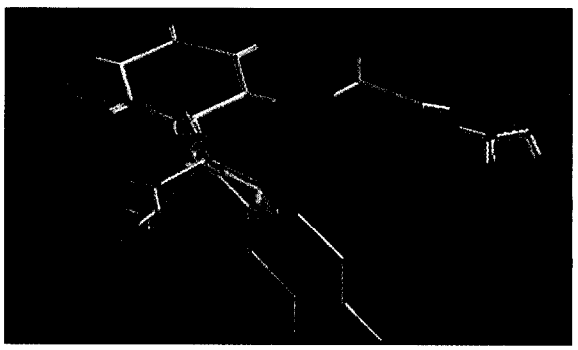

Figure 2. Steric and lipophilic contour plot for model C6 expressed as STDEV×COEFF (contour level: −0.070 red; 0.016 green; −0.029 cyan; 0.035 yellow. Color code: see Table 7). Ligands **3, 26, 29, 31**, and **32** are displayed to help interpretation.

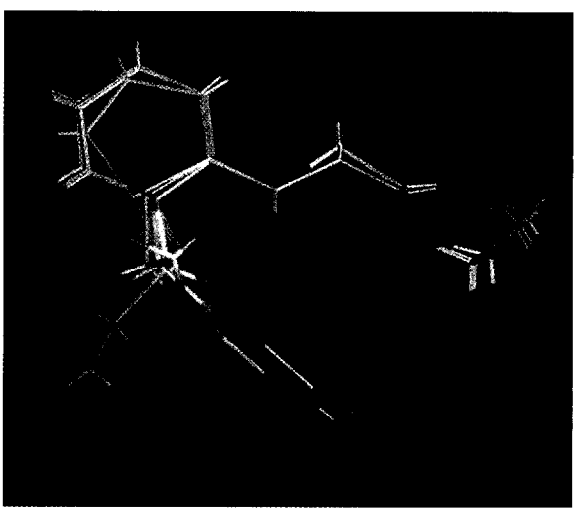

Figure 3. Steric and lipophilic contour plot for model CT5 expressed as STDEV×COEFF (contour level: −0.070 red; 0.030 green; −0.027 cyan; 0.075 yellow. Color code: see Table 7). Ligands **5, 22, 32**, and **33** are displayed to help interpretation.

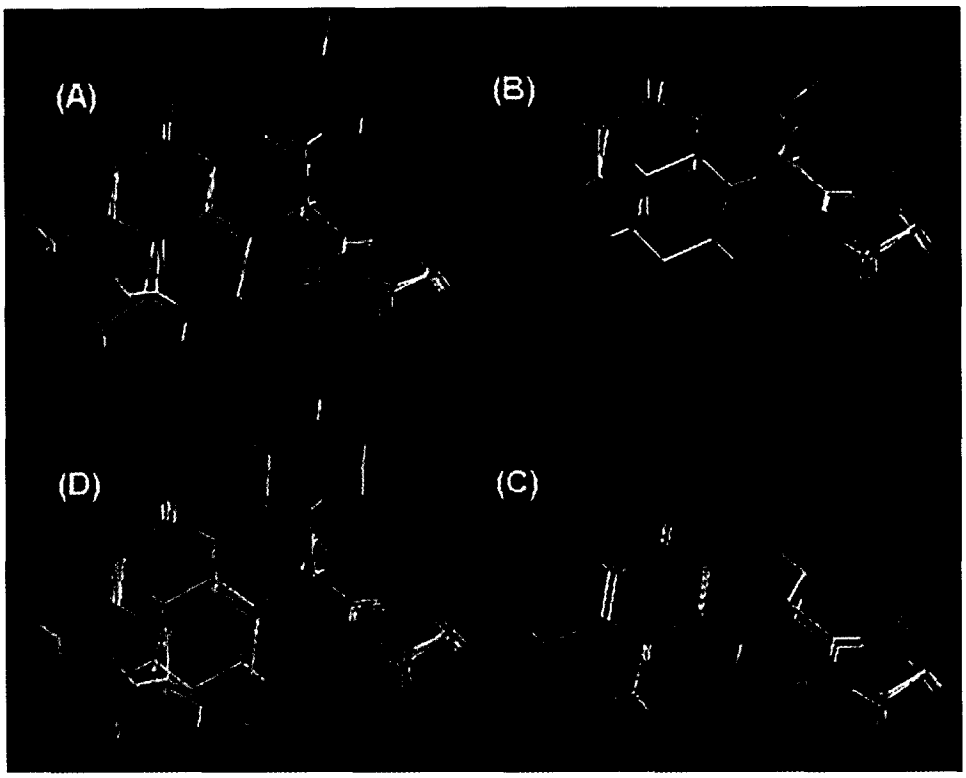

Figure 4. Separated steric (A), electrostatic (B), and lipophilic (C) contour plot for model W7 expressed as STDEV×COEFF (contour level: −0.055 red; 0.040 green; −0.055 magenta; 0.065 white; −0.045 cyan; 0.050 yellow. Color code: see Table 7). Model (D) represents the overlay of the three fields. *Idazoxan* (B, C, D), *Clonidine* (B, D), 2-(9′-*anthryl*)-*imidazoline*[19] (A, D) and ligands **3** (A, D), **5** (C, D), **11** (A, C, D), **36** (A, B, D) are displayed in the maps indicated in parenthesis, to help interpretation.

(hydrophobic or hydrophilic component) fields is accounted for with an interchanging color code. For the sake of clarity, the CoMFA results will be discussed first for the strictly congeneric classes, then for these classes taken together and finally for all the imidazoline derivatives analyzed by us in the present and past studies.[18,19]

Tracizolines

The statistical results of CoMFA for tracizolines are summarized in Table 3. The best correlation was found with the lipophilic field alone (Model T3), all the two-field model combinations giving worse results. Model T3 compares quite well with eq (4) but the significant, albeit small, electronic effect of *para* substituents, suggested by eq (2), was not detected by CoMFA.

The graphical results from model T3 are represented in Figure 1. The yellow zone in the *ortho* region is easily interpretable whereas no simple explanation can be found for the cyan zone close to the *trans* ethenyl bridge.

Cirazolines

The statistical CoMFA results of this series are reported in Table 4. Model C1 agrees with our previous models obtained from a larger set of cirazolines, comprising the low affinity ligands methylated at the carbon of the oxymethylene bridge (compds **36–39**, Table 2). In this step, we have limited our analysis to the cirazoline congeners **3**, **25–35** to avoid a 'flash-light' effect of the

Table 7. Color code of CoMFA isocontour maps in Figures 1–4

Field or field component	Increased affinity	Decreased affinity
Steric field	Green	Red
Electrostatic field (positive charge)	White	Magenta
Electrostatic field (negative charge)	Magenta	White
Lipophilic field (lipophilic component)	Yellow	Cyan
Lipophilic field (hydrophilic component)	Cyan	Yellow

strong field signals from the C-CH_3 region, that would have outshined the others, lighter but significant signals, from other regions.

Even though the best statistical PLS model was that with the steric field alone (C1), a certain influence of the lipophilic field on the activity cannot be ruled out. In fact, when the strong outlier isopropoxy derivative **35** is eliminated from model T3, a statistically significant model was developed also with the lipophilic field alone (Model C4). This is not surprising, since a strong correlation between bulk (steric) and lipophilic substituent properties exist in the analyzed data set.

It is worth stressing that the problem of colinearity might exist also for better designed set of substituents, since the lipophilicity encodes two major contributions, namely a bulk term, accounting for hydrophobic and dispersive forces, and a polar term reflecting electrostatic interactions and hydrogen bonds.[43] A certain extent of correlation between lipophilic and steric (or electrostatic) fields must be expected and should be properly taken into account in any CoMFA model based on combined fields. However, inasmuch as the analysis of the CoMFA contour maps reveals specific features which help interpreting the SAR in a rational way, the use of combined fields should be pursued. Within the limits of the above considerations, a statistically significant model based on the combination of the steric and lipophilic fields was developed (C6), its graphical results being represented in Figure 2.

It is evident that small sized, unbranched and lipophilic substituents can occupy favorable steric/lipophilic regions indicated by the green/yellow zones (compds **3**, **26**, and **31** in Figure 2) whereas unfavorable interactions, due to steric hindrance (red regions), may take place for larger or branched substituents (cps **32** and **29** in Figure 2). The hydrophilic cyan regions could represent unfavorable interactions of lipophilic molecular groups.

Tracizolines plus cirazolines

Table 5 shows the statistical CoMFA results of the two classes taken together (compds **2–9, 19–22, 25–35**). The best PLS models are based on the lipophilic field alone (CT3). Eliminating the isopropoxy congener **35** from model CT3, model CT4, with no better statistics, was produced.

Being based on the same data sets, model CT4 can be compared with the parabolic model in π' of eq (9). The two models show close statistics, and suggest that the lipophilicity is the most important property governing the ligand binding of these two classes of compounds. However, CoMFA is not able to detect a parabolic relationship, due to the intrinsic limitations of PLS, which finds out only linear correlations.[33] This problem, could be partly overcome considering the two-fields model CT6 in which the steric field may be a possible descriptor of the descending part of the parabolic relationship, mainly arising from bulky cirazoline congeners as already observed in the PLS models C1 and C6 and in Figure 2.

The graphical representation of the two-fields PLS model CT6 is shown in Figure 3. The salient results to emerge thereby are: (a) a favorable lipophilic region (yellow) in the *ortho–meta* positions, (b) a favorable steric region (green) inside the aromatic ring and very close to the *ortho* position, (c) many sterically forbidden regions (red) close to molecular fragments of bulky or branched substituents. To help interpreting the above observations, tracizolines **5** and **22** and cirazolines **32** and **33** are on display in Figure 3. A visual comparison of Figures 1–3, referring to the PLS models of separated and merged classes of cirazolines and tracizolines, reveals several common features and prove self-consistency in alignments. Moreover, it must be underlined that in the graphical model of the two classes pooled together (Fig. 3) important field signals, which could not be found in the models of single classes, clearly emerge.

General, inclusive model for imidazoline receptor ligands

In the last step of our CoMFA study, a large set of ligands (59 compounds) constituted of cirazoline and tracizoline derivatives (compds **1–39**) and 20 already reported imidazoline derivatives,[18,19] bearing more drastic structural variations, was examined.

The statistical results of the PLS models obtained for the whole set of ligands are summarized in Table 6.

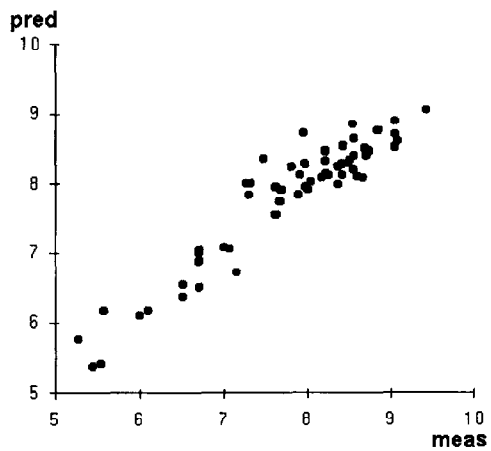

Figure 5. Plot of pK_i values, predicted by general model W7 versus measured values.

Models with acceptable statistics were developed for each molecular field individually (models W1-3), with their pairwise combinations giving slightly improved statistics (models W4-6). The best model, combining all the three fields with very well balanced field contributions (mod. W7), presented fairly good statistics both as fitting ($r^2 = 0.886$, $s = 0.369$ and plot in Figure 5) and predictive values ($q^2 = 0.635$).

The most striking differences between models W and models C, T and CT previously seen, come from the statistically significant influence of the electrostatic field. However, it is worth reminding that the important modeling power of the electrostatic field has been find out in our previous CoMFA study[19] based on about forty imidazoline derivatives that, with the exception of a strong outlier (a chromenone derivative), were now inserted in the final, comprehensive data set. For a better visual inspection, the graphical results of the general inclusive model W7 are presented in Figure 4 both as single and overlaid molecular fields (models A, B, C, and D respectively).

A rapid glance at the graphical steric model A reveals that most of the negative (red) steric signals all around the *ortho* region in CT6 (Fig. 3) were canceled by the stronger field signals in proximity of the methyl substituents on the bridge of low activity cirazolines **36–39**. Also the positive (green) steric signals in model A are reduced and slight differently located compared to model CT6. Interestingly, the steric isocontour map A is quite similar to our early steric model and this is true also for the electrostatic contour map B. Evidently, most of the statistically significant steric and electrostatic information was already present in our previous model.[19] To aid interpretation the following molecules were added to the steric (A), electrostatic (B), and lipophilic (C) isocontour maps:

(A) *Cirazoline* **3** and *m*-CH_3 tracizoline **11** (favorable steric interactions on the green regions); cirazoline congener **36** and 2-(9′-anthryl)imidazoline ($pK_i = 6.00$; unfavorable steric hindrance on the red zones reached by a methyl group and one benzene ring respectively);
(B) *Idazoxan* ($pK_i = 8.37$) and *benazoline* template **1** (favorable electrostatic interactions of the electron rich oxygen and one benzene ring on the magenta regions); clonidine ($pK_i = 6.10$; unfavorable interaction of one electron rich chlorine atom in the white zone);
(C) Methyl substituted tracizolines **5** and **11** (favorable lipophilic interactions on the yellow region); idazoxan (favorable interaction of one oxygen atom in cyan region).

From the previous analysis, it follows that a certain overlay of the signals due to the diverse molecular fields had to be expected. As already underlined, this is not surprising especially for the lipophilic and steric/electrostatic fields, because of the dual nature of lipophilicity which carries both steric (hydrophobic) and electrostatic (polar) components. Indeed, a careful comparative graphical analysis of isocontour maps A, B, and C and even better of the merged field map D, reveals a clear overlay of the lipophilic (yellow) and sterically allowed (green) regions near the *ortho–meta* positions, as well of the electron sensitive (magenta) and hydrophilic (cyan) regions close to one oxygen of idazoxan.

The present case, as several others described in the literature,[44] indicate that the problem of colinearity among statistically significant field signals in CoMFA still awaits for a definite solution.

Despite some objective limitations pointed out in the previous discussion, our results clearly show that an informative CoMFA model can be derived from a large variety of 2-substituted imidazoline derivatives examined in this study. The statistical parameters of the general, inclusive model W7 are quite satisfying both as fitting and predictive power.

The most salient features to emerge from the analysis of the general model W7 are: (a) a favorable lipophilic (steric) interaction close to the *ortho* and *meta* position (3′) of the phenyl ring, (b) a favorable hydrophilic/electronic interaction on the other *meta* region (5′), (c) an unfavorable steric hindrance on two regions, one near and above the imidazoline ring and the other in the distal part of planar polycyclic ligands, (d) an unfavorable high electron density in a zone above the *ortho* region.

The apparent ambiguity in interpreting the influence of the lipophilic and or steric fields in the *ortho–meta* regions should be overcome by a proper design and test of new ligands, especially *meta*-substituted ones. However, when the results from the QSAR analysis leading to eqs (4) and (8) are taken into account a clear indication on the lipophilic nature of the favorable interaction of small sized *ortho* substituents emerges.

To further explore that region with more drastic structural changes and to evaluate the predictive ability of model W7, compounds **40** and **41**, carrying non planar aliphatic substituents, instead of aromatic or heteroaromatic rings characterizing all the ligands examined so far, were synthesized and tested. The pK_i prediction was good for the isopropyl congener **40** (6.85 versus 6.57) whereas a higher deviation was observed for the cyclohexyl congener **41** (8.20 versus 7.26). This was not very surprising, since the cyclohexyl group may carry

additional steric hindrance not taken completely into account by model W7, which was mainly based on more planar ligands.

Finally in order to verify the influence of a structural modification on the *trans* ethenyl or oxymethylene bridge, the *o*-methyl phenethyl derivative **42** was prepared. Its affinity value ($pK_i = 8.37$), is lower than the corresponding cirazoline and tracizoline analogues, **26** and **5** respectively, and it is acceptably well predicted by model W7 ($pK_i = 8.64$).

Conclusions

The use of the molecular lipophilicity potential as a third field in the CoMFA study of imidazoline ligands yielded improved 3-D models, both in statistical and physicochemical terms, and in agreement with QSAR equations, point out an important role of the lipophilic interactions in receptor–ligand binding. The general 3-D CoMFA models are consistent with our previous 3-D models derived from a smaller set of I_2 receptor ligands.

As observed in the past in several SAR studies, the coordinated application of QSAR and 3-D QSAR methods furnishes important information which complement each other giving at the 3-D level a clear picture of the main physicochemical interactions underlying important chemical and biological processes. Our results demonstrate that for congeneric series traditional QSAR approach still yields more valuable and physicochemically better interpretable models than 3-D QSAR methods. However, 3-D QSAR approaches play a decisive and indispensable role when different classes of bioactive molecules have to be examined for the derivation of more general models.

In this respect, the stepwise CoMFA approach is particular efficient allowing a more tuned and depth analysis of congeneric series and thus giving valuable indications also on specific physicochemical forces that could not be detected in a classical, comprehensive CoMFA approach. In the latter, in fact, the molecules under examination are divided, following more or less rigorous sampling criteria, into two subsets, the *training* and the *prediction set*, using the former to derive PLS models and the latter to challenge their predictive ability. This was indeed the philosophy underlining the CoMFA approach which was proposed mainly to overcome some limitations and drawbacks of the QSAR approach when dealing with structurally very diverse molecules.[21] Of course the possibility to carry out a CoMFA study on different sets of molecules in a single step is still one of the main advantages of CoMFA over traditional QSAR, both in terms of efficiency and velocity, but it has to be considered that this procedure could lead to some statistical artifacts and that the contributions of the single classes to the final model could not be correctly perceived and evaluated. In our opinion, as the present and a recent paper[37] clearly prove, the stepwise CoMFA approach should be always pursued when the diverse classes of bioactive molecules under examination show sufficient structural variations and good data spread and distribution. These would be ideal prerequisites to derive informative partial models and easily interpretable general models. The models referring to single classes could be substantially supported and complemented by results from classical QSAR study.

In the more common case of data coming also from classes badly represented, both as structural variations and data spread and distribution, their contribution (if any) to the model could be judged and so the risk of introducing only noise or artifacts to the final model could be kept under control, by eventually excluding those data sets from the final analysis.

We have clearly demonstrated that a comprehensive model, does not result from a mere summation of the information coming from single models derived from strictly congeneric series. Only the most significant statistical signals are in fact retained in the final model and this could be seen as an advantage when the aim of the modeling is to have a general overview of the main physicochemical interactions of the biological process under study. On the other hand, significant insights coming from the analysis of the single classes can be lost. In our opinion, the wealth of useful information coming from all the models have to be judiciously taken into account for the design of new and selective ligands.

Experimental

Chemistry

Tracizolines analogues were synthesized by standard procedures as outlined in Scheme 1. Melting points were taken in glass capillary tubes on a Buchi SMP-20 apparatus and are uncorrected. ^1H NMR spectra were recorded with a Varian EM-390 spectrometer, and chemical shifts are given in parts per million (δ), downfield from tetramethylsilane as the internal standard. Spin multiplicities are given as follows: s (singlet), d (doublet), dd (double doublet), t (triplet), and m (multiplet). The microanalyses were performed in the Microanalytical Laboratory (University of Camerino) for the indicated elements and the results are within ±0.4% of the theoretical values. Chromatographic separations were performed on silica gel columns (Kieselgel 40, 0.040–0.063 mm, Merck) by flash chromatography.

Reactions and product mixtures were routinely monitored by thin-layer chromatography (TLC) on precoated F_{254} silica gel Merck plates.

Physicochemical and spectral data of compounds **4–24** and **40–42** are reported in Table 8.

2-(2′-Chlorostyryl)-4,5-dihydro-1*H*-imidazole oxalate (4). A solution of ethylenediamine (1.16 mL, 17.29 mmol) in dry toluene (5 mL) was added dropwise to a mechanically stirred solution of 2 M trimethylaluminum (8.65 mL, 17.29 mmol) in dry toluene (14.3 mL) at 0 °C in a nitrogen atmosphere. After being stirred at room

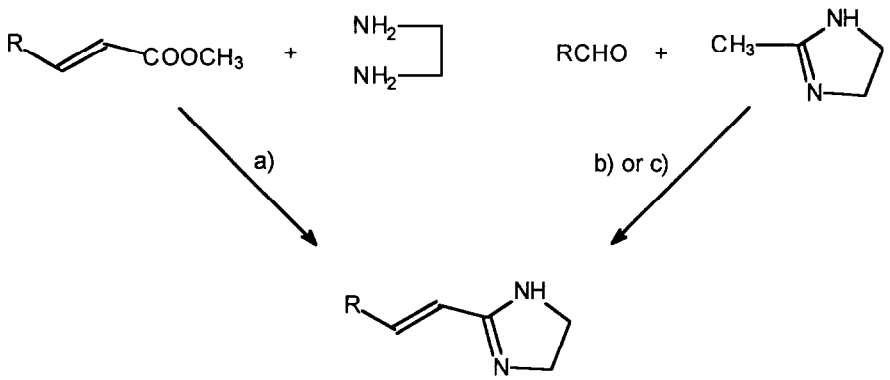

Scheme 1. *Reagents and conditions*: (a) $Al(CH_3)_3$, toluene: compounds **4–6, 12, 14, 15, 40–42**; (b) Δ, butylformate: compounds **7, 16**,[45] **19, 20, 21**,[47] **22**;[48] Δ, ethylformate: compounds **8**,[45] **10, 11, 13, 24**; (c) Δ, toluene: compound **18**;[46] Δ, benzene: compound **23**.

Table 8. Physicochemical and spectral data of compounds **4–24** and **40–42**

Compd	Formula	Recrystn solvent	mp (°C)[a]	yield (%)	^{1}H NMR (δ)				
					Solvent	NCH_2CH_2N	Cα-H	Cβ-H	Ar-H
4	$C_{11}H_{11}ClN_2 \cdot C_2H_2O_4$	EtOH	206–208	65	$CDCl_3$[b]	3.73 (s)	6.73 (d)	7.42 (d)	7.20–7.66 (m)
5	$C_{12}H_{14}N_2 \cdot C_2H_2O_4$	EtOH	210–211	31	$CDCl_3$[b]	3.71 (s)	6.60 (d)	7.36 (d)	7.11–7.55 (m)
6	$C_{12}H_{14}N_2O \cdot C_2H_2O_4$	EtOH/Et_2O	198–199	23	$CDCl_3$[b]	3.72 (s)	6.80 (d)	7.51 (d)	6.80–7.58 (m)
7	$C_{11}H_{11}N_3O_2 \cdot HCl$	2-PrOH	271–272	47	CD_3OD[b]	3.68 (s)	6.60 (d)	7.68 (d)	7.49–8.09 (m)
8	$C_{11}H_{12}N_2O \cdot HCl$	EtOH	235–237	44	CD_3OD	3.98 (s)	6.98 (d)	7.95 (d)	6.80–7.52 (m)
9	$C_{11}H_{13}N_3 \cdot 2HCl$	EtOH/Et_2O	251–252	10	CD_3OD[b]	3.99 (s)	6.55 (d)	7.98 (d)	6.65–7.49 (m)
10	$C_{11}H_{11}N_5 \cdot C_2H_2O_4$	EtOH	190–191	29	CD_3OD	4.01 (s)	6.84 (d)	7.96 (d)	7.23–7.80 (m)
11	$C_{12}H_{14}N_2 \cdot C_2H_2O_4$	EtOH	213–215	33	DMSO	3.91 (s)	6.88 (d)	7.83 (d)	7.20–7.60 (m)
12	$C_{11}H_{11}ClN_2 \cdot C_2H_2O_4$	EtOH	220–221	59	$CDCl_3$[b]	3.72 (s)	6.69 (d)	7.06 (d)	7.25–7.45 (m)
13	$C_{11}H_{11}IN_2 \cdot C_2H_2O_4$	EtOH/Et_2O	240–241	55	$CDCl_3$[b]	3.72 (s)	6.79 (d)	7.41 (d)	7.16–7.72 (m)
14	$C_{12}H_{14}N_2 \cdot C_2H_2O_4$	EtOH	223–224	38	$CDCl_3$[b]	3.71 (s)	6.68 (d)	7.10 (d)	7.11–7.42 (m)
15	$C_{12}H_{14}N_2O \cdot C_2H_2O_4$	EtOH	220–221	12	$CDCl_3$[b]	3.69 (s)	6.58 (d)	7.06 (d)	6.84–7.46 (m)
16	$C_{11}H_{12}N_2O \cdot HCl \cdot 0.5H_2O$	H_2O	223–225	19	CD_3OD	3.96 (s)	6.53 (d)	7.67 (d)	6.81–7.63 (m)
17	$C_{11}H_{13}N_3 \cdot 2HCl$	EtOH/Et_2O	241–242	20	CD_3OD[b]	4.03 (s)	6.83 (d)	7.79 (d)	7.42–7.88 (m)
18	$C_{11}H_{11}N_3O_2 \cdot HCl$	2-PrOH	244–245	32	CD_3OD[b]	4.04 (s)	6.98 (d)	7.81 (d)	7.88–8.37 (m)
19	$C_{10}H_{11}N_3 \cdot C_2H_2O_4$	EtOH/Et_2O	178–179	20	DMSO	3.89 (s)	7.20 (d)	7.85 (d)	7.45–8.72 (m)
20	$C_9H_{11}N_3 \cdot C_2H_2O_4$	2-PrOH	186–187	13	DMSO	3.81 (s)	6.31 (d)	7.60 (d)	6.20–7.19 (m)
21	$C_9H_{10}N_2O \cdot C_2H_2O_4$	EtOH/Et_2O	194–195	28	$CDCl_3$[b]	3.70 (s)	6.56 (d)	6.97 (d)	6.42–7.43 (m)
22	$C_9H_{10}N_2S \cdot C_2H_2O_4$	EtOH/Et_2O	205–206	16	$CDCl_3$[b]	3.70 (s)	6.51 (d)	7.26 (d)	6.88–7.33 (m)
23	$C_{15}H_{14}N_2 \cdot C_2H_2O_4$	MeOH	243–244	11	$CDCl_3$[b]	3.76 (s)	6.79 (d)	7.91 (d)	7.42–8.20 (m)
24	$C_{15}H_{14}N_2 \cdot C_2H_2O_4$	MeOH	218–220	48	CD_3OD	4.04 (s)	6.89 (d)	7.92 (d)	7.51–8.13 (m)
40	$C_8H_{14}N_2 \cdot C_2H_2O_4 \cdot 0.25H_2O$	2-PrOH/Et_2O	163–165	10	CD_3OD	3.97 (s)	6.10 (d)	7.02 (dd)	
41	$C_{11}H_{18}N_2 \cdot C_2H_2O_4 \cdot 0.25H_2O$	2-PrOH	159–160	15	DMSO	3.81 (s)	6.09 (d)	7.05 (dd)	
42	$C_{12}H_{16}N_2 \cdot C_2H_2O_4 \cdot 0.5H_2O$	2-PrOH	146–147	56	DMSO: 2.30 (3H, s, $ArCH_3$); 2.75 (2H, m, $CH_2C=N$); 2.95 (2H, m, $ArCH_2$); 3.81 (4H, s, NCH_2CH_2N); 7.10–7.30 (4H, m, Ar-H)				

[a]The heating rate was about 1 °C min^{-1}.
[b]^{1}H NMR of free base is reported.

temperature for 1 h, the solution was cooled to 0 °C and a solution of methyl 2-chlorocinnamate[49] (1.7 g, 8.65 mmol) in dry toluene (12 mL) was added dropwise. The reaction mixture was refluxed for 45 min, cooled to 0 °C, and quenched cautiously with MeOH (4 mL) followed by water (0.7 mL). After addition of $CHCl_3$ (30 mL), the mixture was refluxed for 1 h at 100 °C to ensure the precipitation of the aluminum salts. The mixture was dried over Na_2SO_4, filtered, diluted with $CHCl_3$, and washed twice with water. The organic layer was extracted with 2 N HCl. The aqueous layer was made basic with 2 N NaOH and extracted with Et_2O. The organic layer was dried over Na_2SO_4, filtered, and evaporated in vacuo to give the free base as a white solid (1.16 g, mp 131–2 °C, 65% yield). The free base was transformed into the oxalate salt by addition of oxalic acid in dry ether solution. Anal. ($C_{13}H_{13}ClN_2O_4$) C, H, N.

Similarly, compounds **5, 6, 12, 14, 15, 40–42** were obtained from the appropriate cinnamic acid methyl esters,[49–52] β-cyclohexylacrilic acid methyl ester,[53] 4-methyl-2-pentenoic acid methyl ester[54] and β-(2-tolyl)-propionic acid methyl ester prepared as previously described.[55]

2-(2′-Nitrostyryl)-4,5-dihydro-1*H*-imidazole hydrochloride (7). A solution of 2-nitrobenzaldehyde (2.0 g, 13.23 mmol), 2-methylimidazoline (0.93 g, 10.99 mmol) and butylformate (9.5 mL, 83.1 mmol) was heated at 90 °C for 3 h. Upon cooling the volatile components of the reaction mixture were evaporated under reduced pressure to give a residue, which was taken up in 2-PrOH (100 mL) and concd HCl (12 mL). The resulting solution was evaporated, and the residue was recrystallized. Anal. ($C_{11}H_{12}ClN_3O_2$) C, H, N.

Similarly, compounds **16**,[45] **19, 20, 21**,[47] and **22**[48] were obtained from the appropriate, commercially available aldehydes. The same procedure was adopted to prepare compounds **8**,[45] **10, 11, 13**, and **24**, using ethylformate instead of butylformate.

2-Azidobenzaldheyde. This product was prepared as previously described.[56]

4-Iodobenzaldehyde. This product was prepared by a procedure slightly different from that reported in lit.[57] Acetic anhydride (8 mL) and 4-iodotoluene (1 g, 4.6 mmol) were placed in a three-necked, round-bottomed flask provided with a mechanical stirrer, dropping funnel, and a thermometer, surrounded by an ice-salt bath. Concentrated sulfuric acid (1.6 mL) was slowly added to this stirred solution. After cooling to 0 °C, a solution of chromium trioxide (2 g, 0.02 mmol) in acetic anhydride (9 mL) was slowly added at such a rate that the temperature did not exceed 10 °C, and stirring was continued for 2 h at 5–10 °C in an ice-water bath after the addition was complete. The content of the flask was poured into H_2O and ice. The solid was filtered and washed with sodium hydrogen carbonate solution and water. The 4-iodobenzaldiacetate obtained was recrystallized from EtOH (1 g; mp 98–99 °C; 65% yield).

A mixture of 4-iodobenzaldiacetate (1 g, 3.0 mmol), H_2O (2.2 mL), EtOH (2.2 mL), and concentrated H_2SO_4 (0.22 mL) was refluxed for 30 min. The mixture was diluted with water and kept in an ice bath for a few hours. The solid was filtered, washed with cold water, and dried (0.4 g; mp 76 °C; 58% yield).

2-(α-Naphthylstyryl)-4,5-dihydro-1*H*-imidazole oxalate (23). A solution of α-naphthylaldehyde (2.2 g, 12.81 mmol) and 2-methylimidazoline (0.95 g, 10.67 mmol) in dry benzene (15 mL) was heated under reflux in a Dean–Stark apparatus and the water formed continuously removed for 18 h. The benzenic solution was evaporated, and the residue was purified on silica gel column using cyclohexane/AcOEt/EtOH/33% NH_4OH (3/1/1/0.6) as eluent to give a solid (0.17 g; mp 134–5 °C; 11% yield). This product was characterized as oxalate salt. Anal. ($C_{17}H_{16}N_2O_4$) C, H, N. Similarly, compound **18**[46] was obtained starting from 4-nitrobenzaldheyde using toluene as reaction solvent.

2-(2′-Aminostyryl)-4,5-dihydro-1*H*-imidazole dihydrochloride (17). A solution of 2-(4-nitrostyryl)-4,5-dihydro-1*H*-imidazole (**18**) (0.5 g, 2.3 mmol) in MeOH (20 mL) was hydrogenated for 0.5 h at room temperature under pressure (30 psi) using Ni/Raney as catalyst. Following catalyst removal, the evaporation of the solvent gave an oil which was purified on silica gel column using as eluent cyclohexane/AcOEt/MeOH/33% NH_4OH (3/7/1.5/0.1). The free base was characterized as hydrochloride salt. Anal. ($C_{11}H_{15}Cl_2N_3$) C, H, N. Similarly, compound **9** was obtained starting from nitroderivative **7**.

2-D QSAR study

Cross-validated multilinear regression was carried out with the c-QSAR software (Biobyte Corp., Claremont, U.S.A). Electronic parameters (σ, F, and R), Charton steric parameters (ν), molar refractivity (MR), and hydrophobic constant (π) were taken from standard compilations.[28,58]

Molecular modeling and CoMFA study

Molecular models of protonated imidazoline receptor ligands were constructed with standard bond distances and angles using SYBYL (Ver. 6.3) software (Tripos Assoc. St. Louis, MO, U.S.A) running on a Silicon

Graphics Indigo2 R4400 workstation. Full geometry optimization was performed with the AM1 Hamiltonian using the parameter set reported in the MOPAC (ver. 6.0) suite of programs.[59]

The partial Mulliken atomic charges from AM1 calculations were used in the CoMFA study. The conformational analysis was carried out with the SYSTEMATIC SEARCH option of SYBYL, screening the conformational space of each torsion angle at 30° increments. All the generated conformers were optimized by the Tripos standard Force Field (MAXIMIN2)[60] and those retained for the subsequent fit and CoMFA analysis were reoptimized by AM1. The molecular superimpositions for CoMFA were made with the RIGID-FIT option of SYBYL.

The CoMFA study was carried out using the QSAR module of SYBYL. Default setting were used in the analyses, except for the 'drop-electrostatic' option which was set to 'NO'. The steric and electrostatic interaction energies were calculated on grid points of a regularly-spaced 3-D lattice with an sp^3 carbon probe atom having a charge of +1 and a van der Waals radius of 1.52 Å. The MLP was calculated by the method of Gaillard et al.;[36] due to the lack of the fragment value for the azido group, compound **10** could not be included in the analysis. The grid size had a resolution of 2 Å and the region dimensions were defined with the 'molecular volume' automatic mode. CoMFA was performed in two successive steps. In a first analysis, using 5 to 8 components and a number of cross-validation groups equal to the number of compounds, the optimal number of components (ONC) was determined. The ONC is that number of components which yielded the highest cross-validated r^2_{cv} (q^2) values which is defined as $q^2 = (SD-PRESS)/SD$ where SD is the sum of squares of deviations of the observed values from their mean and PRESS is the prediction error sum of squares.

In the second step, the analysis was repeated without cross-validation using the ONC previously determined (see text). The results of the last analysis were used to produce the final 3-D QSAR models from which the coefficient isocontour maps depicted in Figures 1–4 were drawn. The predictive and fitting capability of the models were measured by the cross-validated r^2 (q^2) and r^2 (and s, standard deviation), respectively.

Pharmacology

Affinity (expressed as $pK_i \pm SD$) for I_2 and α_2 receptors of test compounds was assessed by measuring their ability to displace [^{3}H]-idazoxan from rabbit kidney and [^{3}H]-clonidine from rat cortex, respectively, as previously described.[18]

Acknowledgements

The financial support from CNR (Rome) and MURST (Rome) is gratefully acknowledged.

References and Notes

1. Bousquet, P. *Neurochem. Int.* **1997**, *30*, 3.

2. *The Imidazoline Receptor: Pharmacology, Functions, Ligands, and Relevance to Biology and Medicine*; Reis, D. J.; Bousquet, P.; Parini, A., Eds.; *Ann. N. Y. Acad. Sci.* **1995**, Vol. 763.

3. Molderings, G. J. *Drugs of the Future*, **1997**, *22*, 757.

4. Michel, M. C.; Ernsberger, P. *Trends Pharmacol. Sci.* **1992**, *13*, 369.

5. Tesson, F.; Prip-Buus, C.; Lenoine, A.; Pegorier, J. P.; Parini, A. *J. Biol. Chem.* **1991**, *266*, 155.

6. van Zwieten, P. A. *J. Hypertens.* **1997**, *15*, 117 and S3.

7. Chu, T. C.; Socci, R. R.; Ogidigben, M. J.; Potter, D. E. *J. Ocul. Pharmacol. Therap.* **1997**, *13*, 489.

8. Olmos, G.; Alemany, R.; Escriba, P. V.; Garcia-Sevilla, J. A. *Br. J. Pharmacol.* **1994**, *111*, 997.

9. LeBrigand, L.; Virsolvy, A.; Peyrollier, K.; Manechez, D.; Godfroid, J. J.; Guardiola Lemaitre, B.; Bataille, D. *Brit. J. Pharmacol.* **1997**, *122*, 786.

10. Molderings, G. J.; Donecker, K.; Burian, M.; Simon, W. A.; Schroeder, D. W., Göthert, M. *J. Pharmacol. Exp. Ther.* **1998**, *285*, 170.

11. Hohage, H.; Hess, K.; Jahl, C.; Greven, J.; Schlatter, E. *Clin. Nephrol.* **1997**, *48*, 346.

12. Ohara-Imaizumi, M.; Kumakura, K. *Cell. Mol. Neurobiol.* **1992**, *12*, 273.

13. Molderings, G. J.; Schmidt, K.; Bönisch, H.; Göthert, M. *Naunyn-Schmied Arch. Pharmacol.* **1995**, *354*, 245.

14. Nutt, D. J.; French, N.; Handley, S.; Hudson, A.; Husband, S.; Jackson, H.; Jordan, S.; Lalies, M. D.; Lewis, J.; Lione, L.; Mallard, N.; Prat, J. *Ann. N. Y. Acad. Sci.* **1995**, *763*, 125.

15. Musgrave, I. F.; Krautwarst, D.; Schultz, G. *Clin. Exp. Pharmacol. Physiol.* **1996**, *23*, 990.

16. Drnsbezrger, P.; Friedman, J. E.; Koletsky, R. J. *J. Hypertension* **1997**, *15*, S9.

17. Brasili, L.; Pigini, M.; Bousquet, P.; Carotti, A.; Dontenwill, M.; Giannella, M.; Moriconi, R.; Piergentili, A.; Quaglia, W.; Tayebati, K. S. In *Perspective in Receptor Research*; Giardinà, D.; Piergentili, A.; Pigini, M., Eds.; Elsevier: Amsterdam, 1996; 361–373.

18. Pigini, M.; Bousquet, P.; Carotti, A.; Dontenwill, M.; Giannella, M.; Moriconi, R.; Piergentili, A.; Quaglia, W.; Tayebati, S. K.; Brasili, L. *Bioorg. Med. Chem.* **1997**, *5*, 833.

19. Carrieri, A.; Brasili, L.; Leonetti, F.; Pigini M.; Giannella, M.; Bousquet, P.; Carotti, A. *Bioorg. Med. Chem.* **1997**, *5*, 843.

20. Kubinyi, H. *QSAR: Hansch Analysis and Related Approaches*, VHC: Weinheim, 1993.

21. Cramer, R. D.; Patterson, D. E.; Bunce, J. D. *J. Am. Chem. Soc.* **1988**, *110*, 5959.

22. Kneubühler, S.; Thull, U.; Altomare, C.; Carta, V.; Gaillard, P.; Carrupt, P.-A.; Carotti, A.; Testa, B. *J. Med. Chem.* **1995**, *38*, 3874.

23. Carrieri, A.; Altomare, C.; Barreca, M. L.; Contento, A.; Carotti, A.; Hansch, C. *Il Farmaco*, **1994**, *49*, 573.

24. Altomare, C.; Carotti, A.; Cellamare, S.; Carrupt, P.-A.; Testa, B. *Chirality* **1993**, *5*, 527.

25. Greco, G.; Novellino, E.; Silipo, C.; Vittoria, A. *Quant. Struct. -Act. Relat.* **1992**, *11*, 461.

26. Debnath, A. K.; Hansch, C.; Kim, H. K.; Martin, Y. C. *J. Med. Chem.* **1993**, *36*, 1007.

27. C-Log P Mac vers. 2. 0, 1996, Biobyte Corp., Claremont, CA, USA.

28. Hansch, C.; Leo, A.; Hoeckman, D. *Exploring QSAR*, ACS, Washington, 1995, vol 2.

29. Carotti, A.; Altomare, C. *Chim. & Ind.*, **1995**, *77*, 13 and references therein.

30. Selassie, C. D.; Klein, T. E. In *3D QSAR in Drug Design: Theory, Methods and Applications*; Kubinyi, H. Ed.; Escom: Leiden, 1993; pp 257–275.

31. Cramer, R. D.; De Prierst, S. A.; Patterson, D. E.; Hect, P. 'The developing practice of Comparative Molecular Field Analysis' in ref,[30] pp 443–485.

32. Dunn, III W. J.; Wold, S.; Edlund, U.; Helberg, S. *Quant. Struct. -Act. Relat.* **1984**, *3*, 131.

33. Wold, S.; Johansson, E.; Cocchi, M. 'PLS-Partial Least Squares Projections to Latent Structures' in ref.,[30] pp 523–549.

34. Cramer, III R. D; Bunce, J. D.; Patterson, D. E. *Quant. Struct. -Act. Relat.* **1988**, *7*, 18.

35. Thibaut, U. 'Applications of CoMFA and Related 3D-QSAR Approaches' in ref.,[30] pp 661–696.

36. Gaillard, P.; Carrupt, P.-A.; Testa, B.; Boudon, A. *J. Comput. -Aided Mol. Des.* **1994**, *8*, 83.

37. Gaillard, P.; Carrupt, P.-A.; Testa, B.; Schambel, P. *J. Med. Chem.* **1996**, *39*, 126.

38. Testa, B.; Carrupt, P.-A.; Gaillard, P.; Billois, F.; Weber, P. *Pharm. Res.* **1996**, *13*, 126.

39. Stewart, J. J. P. *J. Comput. -Aided Mol. Des.* **1990**, *4*, 1.

40. Wold, S.; Eriksson, L. In *Chemometric Methods in Molecular Design*; van de Waterbeemd, H., Ed.; VCH: Weinheim, 1996, pp 309–318.

41. Folkers, G.; Merz, A.; Rognan, D. 'CoMFA scope and limitations' in ref.,[30] pp 583–618.

42. Wold, S. 'PLS for Multivariate Linear Modeling' in ref.,[40] pp 195–218.

43. Testa, B.; Carrupt, P.-A.; Gaillard, P.; Tsai, R. S. Intramolecular Interactions Encoded in Lipophilicity. In *Lipophilicity in Drug Action and Toxicology*; Pliska, V.; Testa, B.; van der Waterbeemd, H., Eds.; VCH: Weinheim, 1997, pp 49–71.

44. Carrupt, P.-A.; Gaillard, P.; Billois, F.; Weber, P.; Testa, B.; Meyer, L.; Perez, S. in ref,[43] pp 195–217.

45. McFarland, J. W.; Howes, Jr. H. L. *J. Med. Chem.* **1972**, *15*, 365.

46. Shvekhgeimer, G. A.; Gorbatov, E. I.; Tyurin, V. D. *Zh. Org. Khim.* **1971**, *7*, 815; *Chem. Abstr.* **1971**, *75*, 35881p.

47. Chas. Pfizer & Co., Inc. Neth. Appl. 6, 607, 037; *Chem. Abstr.* **1968**, *68*, 49640b.

48. McFarland, J. W.; Conover, L. H.; Howes, Jr. H. L.; Lynch, J. E.; Chisholm, D. R.; Austin, W. C.; Cornwell, R. L.; Danilewicz, J. C.; Courtney, W.; Morgan, D. H. *J. Med. Chem.* **1969**, *12*, 1066.

49. Pagani, G.; Caccialanza, G.; Montanari, L. *Il Farmaco-Ed. Sci.* **1973**, *28*, 231 and ref. therein.

50. Kolsaker, P.; Ellingsen, P. O. *Acta Chem. Scand. B* **1979**, *33*, 138.

51. Kolsaker, P.; Bailey, P. S. *Acta Chem. Scand.* **1967**, *21*, 537.

52. de la Mare, P. B. D.; Wilson, M. A.; Rosser, M. J. *J. Chem. Soc., Perkin Trans. 2* **1973**, 1480.

53. Sarbbani, S. G. S. *J. Chem. Soc.* **1928**, 54.

54. Adamson, D. W. *J. Chem. Soc.* **1950**, 885 and ref. therein.

55. House, H. O.; Melillo, D. G.; Sauter, F. J. *J. Org. Chem.* **1973**, *38*, 741.

56. Ardakani, M. A.; Smalley, R. K.; Smith, R. H. *J. Chem. Soc., Perkin Trans. 1* **1983**, 2501.

57. Baker, J. W.; Hopkins, H. B. *J. Chem. Soc.* **1949**, 1089.

58. van de Waterbeemd, H.; Testa, B. *Advances in Drug Research*; Testa, B., Ed.; Academic Press: New York, 1987, vol. 16, pp 85–225.

59. MOPAC 6. 0 is available from QCPE (506).

60. Clark, M.; Cramer, R. D.; Van Opdenbasch, N. *J. Comput. Chem.* **1989**, *10*, 982.